RAPID COMMUNICATIONS

PHYSICAL REVIEW B VOLUME 51, NUMBER 2 1 JANUARY 1995-II

Electronic band structure of the superconductor Sr_2RuO_4

Tamio Oguchi

Department of Materials Science, Hiroshima University, 1-3-1 Kagamiyama, Higashi-Hiroshima 724, Japan

(Received 28 September 1994; revised manuscript received 8 November 1994)

A local-density electronic-band-structure calculation was performed for a recently discovered non-copper-layered perovskite superconductor, Sr_2RuO_4. It was found that the electronic structure near the Fermi energy is essentially described by antibonding bands of the Ru $d\varepsilon$ and O $p\pi$ states. Although two holes in the bands are predominantly situated in a $d\varepsilon(xy)$-$p\pi$ state in the ab plane, the hole occupations in the other $d\varepsilon$-$p\pi$ states vertical to the plane are not negligibly small, possibly in conjunction with the smallness of tetragonal distortion of the RuO_6 octahedron. Associated with the antibonding $d\varepsilon$-$p\pi$ bands, the density of states at the Fermi energy is relatively high (4.36 states/eV cell) but not enough to account for the observed specific-heat constant γ_{exp} and temperature-independent magnetic susceptibility χ_{exp}. We found a large Stoner factor, which may explain most of the mass enhancement involved in χ_{exp}. Certain similarities and dissimilarities in the electronic properties to the cuprate superconductors are discussed.

Since the observation of superconductivity in $La_{2-x}Ba_xCuO_4$ (LBCO) by Bednorz and Müller,[1] several superconducting copper oxides have been discovered, forming a new class of superconductors with remarkably high transition temperatures, namely high-temperature superconductors (HTSC's). The most peculiar feature commonly seen in HTSC's is that all of them have a layered perovskite crystal structure containing a planar CuO_2 network. It has been well recognized that, in the CuO_2 planes, significantly large hybridization between the Cu $d(x^2-y^2)$ and O $p\sigma$ states is a crucial factor in describing the electronic structure as well as the strong correlation on the Cu site. A number of efforts have been made for some years to find a layered perovskite superconductor without copper but no one had succeeded until a very recent discovery. Maeno *et al.*[2] discovered superconductivity at 0.93 K in a non-copper-oxide, Sr_2RuO_4, with the same crystal structure as LBCO. This discovery would provide us with another opportunity to verify whether the microscopic understanding of the HTSC compounds is valid for a wider range of oxide superconductors.

In this paper, we calculate the electronic band structure of Sr_2RuO_4 to explore the similarity and dissimilarity in the electronic structure by comparison with ordinary copper oxide HTSC's. Our results show that there exists large hybridization between the Ru d and O p states in Sr_2RuO_4. An important difference from the cuprate HTSC's is that relevant orbitals to the states near the Fermi energy (E_F) are Ru $d\varepsilon$ and O $p\pi$, instead of Cu $d(x^2-y^2)$ and O $p\sigma$ states.

The present calculation is based on the local-density approximation (LDA) to density-functional theory. We use a self-consistent, scalar-relativistic version of the linear-augmented-plane-wave (LAPW) method[3] and the Hedin-Lundqvist exchange correlation.[4] The potential and charge density are expanded in the whole space with plane waves and inside the muffin-tin spheres with spherical waves, by following Soler and Williams' prescription.[5] A typical number of plane waves used in the computation is 962. The self-consistency is achieved by the linear tetrahedron method with 13 uniformly-distributed **k** points in the irreducible Brillouin zone.

The observed crystal structure of Sr_2RuO_4 is the K_2NiF_4 type with the $I4/mmm$ space group.[6] The fractional atomic coordinates are given by Sr (0,0,z(Sr)); Ru (0,0,$\frac{1}{2}$); O(I) (0, $\frac{1}{2}$,0); O(II) (0,0,z(O)). No structural transition from tetragonal symmetry has been detected up to 5 K.[2] This may be an important dissimilarity to LBCO or $La_{2-x}Sr_xCuO_4$ (LSCO). The lattice constants and parameters, $a=3.8603$ Å, $c=12.729$ Å, z(Sr)=0.146 84, and z(O)=0.3381, at 100 K (Ref. 6) are utilized in the calculation. From the crystal data, it can be easily seen that the tetragonal distortion of the RuO_6 octahedron in Sr_2RuO_4 [the atomic distances between the Ru and O atoms are R(Ru-O(I))=1.930 Å and R(Ru-O(II))=2.061 Å] is significantly smaller than that in LBCO [R(Cu-O(I))=1.89 Å and R(Cu-O(II))=2.41 Å].

Figure 1 shows the calculated LAPW electronic band structure of Sr_2RuO_4 along high-symmetry lines of the Brillouin zone. Twelve bands lying below -2 eV are mainly the bonding states of the Ru d and O p orbitals, and the nonbonding states of O p. Three bands crossing the Fermi en-

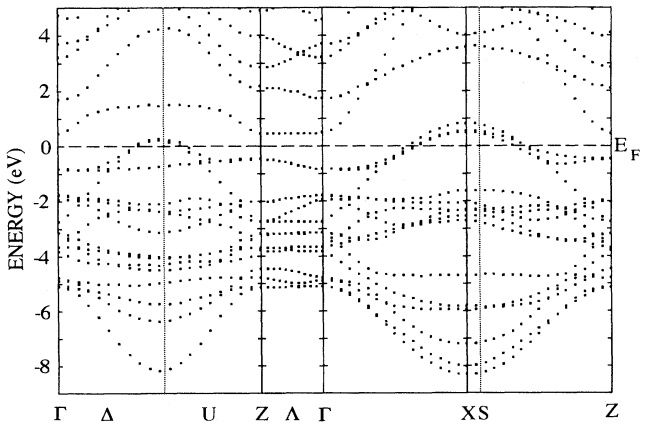

FIG. 1. Calculated energy band structure of Sr_2RuO_4 along high-symmetry lines. A horizontal broken line denotes the Fermi energy.

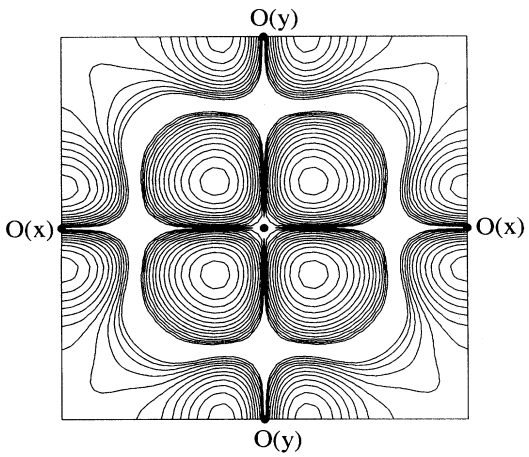

FIG. 2. An ab-plane contour map of the pseudocharge density of the antibonding $d\varepsilon(xy)$-$p\pi$ band at the X point (the 15th band in Fig. 1). Contours of charge density are plotted as $(2)^{n/2}\times 10^{-3}$ electrons/bohr^3 ($n=0,1,\ldots$). A clear node (zero amplitude of the wave function) between the Ru (at center) and four O(I) atoms indicates the antibonding character of the state.

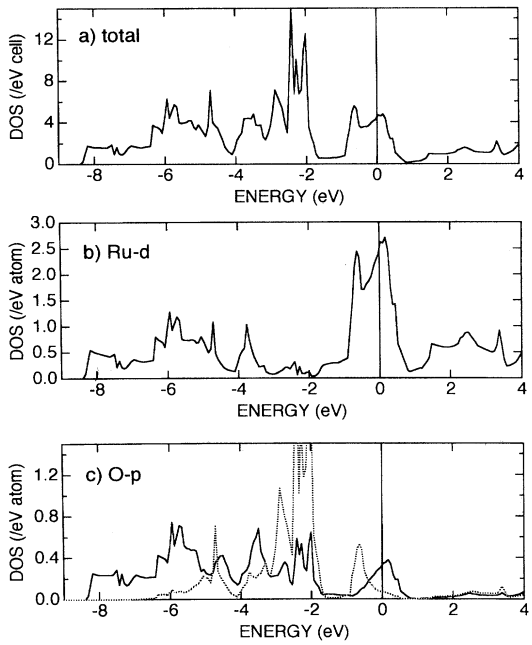

FIG. 3. Calculated density of states (DOS) of Sr_2RuO_4: (a) total DOS, (b) partial Ru d DOS, and (c) partial O p DOS. In panel (c), solid and dotted curves represent the partial p DOS of the O(I) and O(II) atoms, respectively. A vertical line denotes the Fermi energy.

ergy (E_F) have antibonding characteristics of the Ru $d\varepsilon(xy,yz,zx)$ and O $p\pi$ orbitals. Four electrons (or equivalently two holes) remain to occupy these antibonding $d\varepsilon$-$p\pi$ bands. Since the antibonding $d\varepsilon(yz)$-$p\pi$ and $d\varepsilon(zx)$-$p\pi$ bands are fully unoccupied on the Γ-Δ-U-Z lines along the a and b directions, respectively, the two holes are predominantly situated in the $d\varepsilon(xy)$-$p\pi$ band. A typical contour map of the pseudocharge density (a component in the plane-wave representation) of the $d\varepsilon(xy)$-$p\pi$ band is shown in Fig. 2. However, it should be noticed that the hole occupations in the antibonding $d\varepsilon(yz)$-$p\pi$ and $d\varepsilon(zx)$-$p\pi$ bands are not negligibly small. The existence of the hole in the antibonding states vertical to the RuO_2 planes may account for the smallness of the tetragonal distortion of the RuO_6 octahedron. This is in distinct contrast to the situation in La_2CuO_4 (LCO), where one hole is solely in the antibonding band of the Cu $d\gamma(x^2-y^2)$ and O(I) $p\sigma$ orbitals.[7,8] In Fig. 1, the fully unoccupied bands consist of the antibonding states of the Ru $d\gamma(x^2-y^2,3z^2-r^2)$ and O $p\sigma$, and the Sr s and d orbitals. A less dispersive feature can be seen in bands on the Λ line along the c direction, being more clearly so in the Fermi surface as discussed below.

The density of states (DOS) is determined with 30 **k** points in the irreducible Brillouin zone (totally 216 **k** points and 1296 tetrahedra in the full zone). The total DOS and the partial DOS of the Ru d and O p states are plotted in Fig. 3. Note that the partial DOS is evaluated by integrating the charge inside the muffin-tin spheres and its relative magnitude largely depends on the sphere radius assumed (1.1 Å for Ru and 0.6 Å for O). The total DOS at E_F is $N(E_F)=59.4$ states/Ry cell (4.36 states/eV cell), which is much larger than the calculated values (1.1–1.3 states/eV cell) for LCO.[7,8] As shown in the partial DOS in Fig. 3, the antibonding states of the Ru $d\varepsilon(xy,yz,zx)$ and O $p\pi$ orbitals mentioned above are just located around E_F forming a relatively high DOS peak.

The present $N(E_F)$ value corresponds to the temperature-linear coefficient in the specific heat γ_{band} of 10.3 mJ/K^2 mol and the Pauli paramagnetic susceptibility χ_{band} of 1.41×10^{-4} emu/mol. The observed results on the normal-state properties of sintered polycrystalline samples show that the specific-heat constant is $\gamma_{\text{exp}}=39$ mJ/K^2 mol and the temperature-independent component of the magnetic susceptibility is $\chi_{\text{exp}}=9.7\times 10^{-4}$ emu/mol, giving the Wilson ratio of $R_W=1.8$.[2] Both quantities are significantly enhanced about several times from the LDA band value. The mass enhancement in γ is much greater than that of RuO_2 rutile, of which the electronic structure could be interpreted as of an ordinary metal.[9]

To get insight into the origin of the enhancement, the Stoner factor is evaluated by calculating the effective exchange-correlation integral I within the local-spin-density approximation (LSDA).[10] The exchange-correlation integral for Sr_2RuO_4 is found to be $I=187$ meV and leads to the susceptibility enhancement $[1-N(E_F)I]^{-1}$ of 5.4, which is comparable to the obtained enhancement $\chi_{\text{exp}}/\chi_{\text{band}}=6.9$ in the susceptibility. On the other hand, we should expect certain amounts of electron-phonon and electron-correlation effects, which contribute to the specific-heat mass enhancement $\gamma_{\text{exp}}/\gamma_{\text{band}}=3.8$. Considering the low superconducting transition temperature, it may not be plausible to speculate that the electron-phonon interaction gives the major contribution to the specific-heat mass enhancement.

The calculated Fermi surface is drawn in Fig. 4. Three sheets of the Fermi surface as expected from the band structure in Fig. 1 are all associated with the antibonding $d\varepsilon$-$p\pi$ states. Two of them are electron cylinders around the

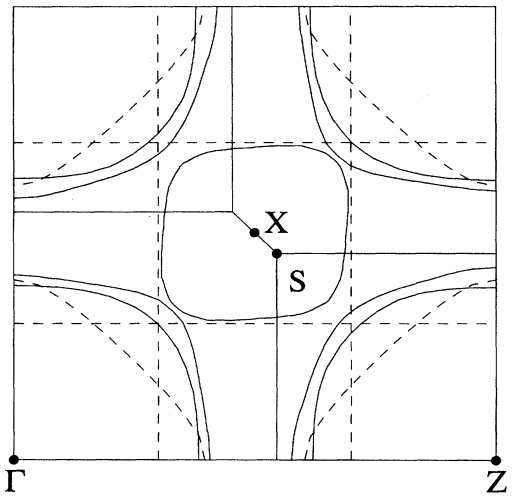

FIG. 4. Calculated Fermi surface of Sr_2RuO_4 in the extended Brillouin zone scheme (solid curves). Two almost-degenerate cylindrical sheets around Γ and Z are electron surfaces and another cylindrical sheet around X is a hole surface. Broken curves indicate the Fermi surface derived from the nearest-neighbor tight-binding model.

Λ line and the remaining one is an X-centered hole cylinder. The cylindrical shape of the Fermi surfaces implies a two-dimensional nature of the electronic properties. A rough fitting of the bonding and antibonding $d\varepsilon$-$p\pi$ bands to a nearest-neighbor tight-binding (TB) model can be achieved by setting four parameters: orbital-energy differences, $E(d\varepsilon)-E(\mathrm{O(I)}\text{-}p\pi)=1.5$ eV and $E(d\varepsilon)-E(\mathrm{O(II)}\text{-}p\pi)=0.0$ eV, and hopping integrals, $pd\pi(d\varepsilon, \mathrm{O(I)}\text{-}p\pi)=1.5$ eV and $pd\pi(d\varepsilon, \mathrm{O(II)}\text{-}p\pi)=1.0$ eV. This TB model provides the Fermi surface consisting of two one-dimensional planes normal to k_x and k_y directions, and one two-dimensional cylinder around the Λ line, as drawn in Fig. 4. A comparison of the hopping parameters to those in LCO ($pd\sigma=-1.85$ eV, $pd\pi=0.75$ eV) (Refs. 7 and 11) indicate that the Ru d states are more delocalized than the Cu d. It has been found that inclusion of the other hopping parameters such as $pp\sigma$ and $pp\pi$ between the O p states is necessary for a more accurate description of all the valence bands.

In order to study the anisotropic nature of the Fermi surface in Sr_2RuO_4, the plasma-frequency tensor is calculated as

$$\Omega_p^2=\frac{8\pi e^2}{V_0}\sum_{\mathbf{k},n}\mathbf{v}_n(\mathbf{k})\mathbf{v}_n(\mathbf{k})\,\delta(E_n(\mathbf{k})-E_F), \qquad (1)$$

where $\mathbf{v}_n(\mathbf{k})$ is the group velocity of the nth band and V_0 is the cell volume. Table I lists the calculated $N(E_F)$, Fermi velocity, and plasma-energy tensor for Sr_2RuO_4, together with the results for LSCO ($x=0.15$) and $YBa_2Cu_3O_7$.[12] It is clearly shown in Table I that, among these oxides, Sr_2RuO_4 has the largest anisotropy in the Fermi velocity and the plasma energy. The large anisotropy may explain the observed resistivity ratio $\rho_c/\rho_{ab}=8.5\times10^2$ at a low temperature though nonmetallic behavior is seen in ρ_c at higher temperatures.[2]

TABLE I. Calculated density of states at E_F, Fermi velocity, and plasma energy tensor for Sr_2RuO_4, $La_{1.85}Sr_{0.15}CuO_4$, and $YBa_2Cu_3O_7$.

	Sr_2RuO_4	$La_{1.85}Sr_{0.15}CuO_4$[a]	YBa2CuO$_3$O$_7$[a]	Unit
$N(E_F)$	59.4	28.4	76.0	states/Ry cell
$\langle v_x^2\rangle^{1/2}$	2.3	2.2	1.8	10^7 cm/s
$\langle v_y^2\rangle^{1/2}$	2.3	2.2	2.8	10^7 cm/s
$\langle v_z^2\rangle^{1/2}$	0.21	0.41	0.7	10^7 cm/s
$\hbar\Omega_{pxx}$	4.5	2.9	2.9	eV
$\hbar\Omega_{pyy}$	4.5	2.9	4.4	eV
$\hbar\Omega_{pzz}$	0.40	0.55	1.1	eV

[a]Reference 12.

Finally, we investigate possible spin-orbit effects on the bands of Sr_2RuO_4, which were excluded in the scalar relativistic treatment. The orbital-energy shifts of the three antibonding $d\varepsilon$-$p\pi$ states at the X point due to the spin-orbit interaction are found to be -48 meV, 14 meV, and 25 meV by a perturbative estimation. The resulting reduction in $N(E_F)$ is less than 1%. The spin-orbit effects on the other valence bands where the O p states dominate are much smaller as expected.

Based on the above theoretical observations on the LDA electronic structure of Sr_2RuO_4, we may conclude that Sr_2RuO_4 belongs to a different class from the copper oxide HTSC's, though there exist certain similarities such as the strong d-p hybridization due to the planar network structure. The most important dissimilarity to be remarked is that Sr_2RuO_4 is not a low-carrier metal in the normal state. The hybridization of the Ru $d\varepsilon$ and O $p\pi$ states is crucial for the description of the electronic properties in Sr_2RuO_4. The relatively high DOS at E_F leads to the large Stoner factor, which is comparable to the mass enhancement found in the magnetic susceptibility. It has been also found that the Fermi surface of Sr_2RuO_4 has stronger anisotropy than LSCO and $YBa_2Cu_3O_7$. However, experimental and theoretical information on the electron-phonon interaction, the magnetic excitation, and transport phenomena is still lacking in this new superconductor. Further investigations are clearly necessary to clarify the electronic nature and the mechanism of superconductivity in Sr_2RuO_4 as well as in HTSC's.

The author would like to thank Y. Maeno for discussing his experimental results prior to publication and for a critical reading of the manuscript. He is grateful to N. Hamada for many useful discussions.

[1] J. G. Bednorz and K. A. Müller, Z. Phys. B **64**, 189 (1986).
[2] Y. Maeno, H. Hashimoto, K. Yoshida, S. Nishizaki, T. Fujita, J. G. Bednorz, and F. Lichtenberg, Nature (to be published).
[3] O. K. Andersen, Phys. Rev. B **12**, 3060 (1975).
[4] L. Hedin and B. I. Lundqvist, J. Phys. C **4**, 2064 (1971).
[5] J. M. Soler and A. R. Williams, Phys. Rev. B **40**, 1560 (1989).
[6] L. Walz and F. Lichtenberg, Acta Crystallogr. C **49**, 1268 (1993).
[7] L. F. Mattheiss, Phys. Rev. Lett. **58**, 1028 (1987).
[8] J. Yu, A. J. Freeman, and J. H. Xu, Phys. Rev. Lett. **58**, 1035 (1987).
[9] K. M. Glassford and J. R. Chelikowsky, Phys. Rev. B **49**, 7107 (1994).
[10] J. F. Janak, Phys. Rev. B **16**, 255 (1977).
[11] A. K. McMahan, R. M. Martin, and S. Satpathy, Phys. Rev. B **38**, 6650 (1988).
[12] P. B. Allen, W. E. Pickett, and H. Krakauer, Phys. Rev. B **37**, 7482 (1988).